Materials Physics and Mechanics. 2022;48(2): 289-299
Research article
http://dx.doi.org/10.18149/MPM.4822022_12
Received: November 10, 2021
Accepted: April 5, 2022

STUDY OF POLYLACTIDE 3D-PRINTED SAMPLES WITH DOUBLE-LAYER WEAVE

A.V. Pogrebnoi✉

JSC "Central Research Institute for Machine Building", 4 Pionerskaya St., Korolev, Moscow Region, 141070, Russia

✉ a.v.pogrebnoy@yandex.ru

Abstract. Fused Deposition Modeling method (FDM) is widely used in various fields of science for prototyping and manufacturing of final functional parts. The actual problem of the FDM method is the low bond strength between the layers of printed parts. Proposed 3D-printing method is based on the formation of double-layer weave between polymer threads. An unfilled polylactide (PLA) was used for fabrication of samples to demonstrate the proposed method. PLA samples with double-layer weave obtained by fused deposition modeling method are studied. Characteristics of samples obtained by static tension test are compared. Their structure and fracture mode are investigated. It is found that double-layer weave affects bond strength between layers of 3D-printed samples. The obtained results show that the proposed method in combination with other methods can be implemented for other polymer materials and composites for local reinforcement of printed parts.
Keywords: adhesion, mechanical properties, tensile strength, reinforcement, double-layer weave, fused deposition modeling, polylactide

Acknowledgements*. No external funding was received for this study.*

Citation: Pogrebnoi AV. Study of polylactide 3D-printed samples with double-layer weave. *Materials Physics and Mechanics.* 2022;48(2): 289-299. DOI: 10.18149/MPM.4822022_12.

1. Introduction

Currently, Fused Deposition Modeling (FDM) invented by S. Crump in 1989 is one of the most widespread technologies of additive manufacturing in the world. Thanks to low equipment cost and availability of consumables, FDM finds wide application in various fields of science and technology for the purpose of prototyping and manufacturing final functional parts [1].

The method consists in slicing a 3D computer model of the part into separate layers, each of which is successively printed on a build platform using a print head. The print head moves on a programmed trajectory represented in the form of the set of commands in the *G-code* language. 3D printing uses a thread-like polymer material (filament) as the main build consumable, which is extruded into the print head, heated to the melting temperature, and pressed through a nozzle of set diameter [2].

The FDM method can be applied in aircraft engineering to design aircraft, bulk elements, and other small-batch parts [3-5]. The costs of molding equipment production for the FDM fabrication of wing covering parts can be reduced by 6–7 times [4], while the time of the equipment production can be reduced by 2–4 times [4,5].

In rocket and space structures, the FDM method can be employed to fabricate parts from engineering thermoplastics capable of long-term operation in high load and temperature conditions [6]. Polyetherimide (PEI), polyether ether ketone (PEEK) [9], and their composites are an example of such materials. Despite the need for further tuning of the technology, certain publications note that the FDM method can be used to produce parts during a space flight to solve the task of on-site repair of malfunctioning devices [10,11-12].

Low bond strength between the layers of the printed parts remains one of the most critical shortcomings of the FDM method [13-14,15]. This issue causes delamination of the fabricated parts in the process of cooling and loss of resistance to various gasses and liquids, including organic solvents [16]. Weak adhesion between the layers of the material requires making the part design stronger and more complex, which increases its weight and fabrication time [17].

The performed analysis of the literature showed that the solutions to this issue can be conditionally divided into three groups.

The first group relates to the optimization of the main technological parameters of 3D printing and includes methods aimed at increasing the bond between the layers of FDM products, mainly by reducing the interval between the threads [18-20], shifting the layers relative to the direction of laying the melt threads [21-22], reducing the layer height [23], and increasing the extrusion temperature during 3D printing [21,24].

The second group refers to the provision of external thermal effects on the product during 3D printing and includes methods based on the use of laser, infrared or ultrasonic sources. Thus, in the process of 3D printing, the required area of the part is locally heated to increase the bond between the layers [25].

The third group of methods is based on improving the properties by adding binders and polymer additives, as well as discrete reinforcing fibers to the composition of the building material [26].

An analysis of publications [13-26] showed that none of the known methods is able to significantly increase the strength of the bond between the layers of printed products.

One of the possible reasons could be the use of standard slicing algorithms that cut the digital model of the part into separate flat (2D) layers.

In this regard, it seems interesting to study the case in which 3D printing is carried out not in a plane, but in space, that is alternately in several layers, with the polymer threads interweaving. The simplest example would be a double-layer weave formed between two adjacent layers of the material.

The aim of this work was to study the effect of double-layer weaving on the strength of the bond between the layers of samples obtained by 3D printing.

2. Experimental Part

Samples were obtained from unfilled white polylactide (PLA) with a density of 1.25 g/cm^3 and a filament diameter of 1.75 mm manufactured by REC, Russian Federation. The choice of PLA for the study was because it is the most widely used material for FDM 3D printing [15,25], and a desktop FDM 3D printer can be used to make samples from PLA [15,17,23].

For the purpose of this work, it was extremely important to comply with the specified geometric dimensions of the samples. The equipment had to have a rigid metal body and kinematics that ensured the movement of the print head in the horizontal plane and the vertical movement of the heated build platform.

Therefore, a widely available desktop 3D printer "Flying Bear Ghost 5" (Jinhua Flyingbear Intelligent Technology Co., Ltd, People's Republic of China) with a print area of 255x210x200 mm (length, width, and height) was used to obtain the samples. 3D printing was carried out in the Cartesian coordinate system.

It is common knowledge that the current mechanical test standards of the GOST, ISO or ASTM series were developed for samples obtained by casting, pressing, or machining [17,23]. Due to the lack of a single standard suitable for testing samples with a complex structure obtained by 3D printing, in this research, all samples were made in the form of a rectangular strip 121 mm long, 20.7 mm wide, and 2.8 mm thick. Each sample consisted of 14 layers of material 0.2 mm thick and was printed at a printing speed of 11.7 mm/s on a substrate that ensured reliable contact with the build platform. The same PLA material was used to print the samples and the substrate. The substrate had a thickness of 0.05 mm and was printed at a speed of 33.3 mm/s. Test samples were printed in the amount of 5 pcs in each series and then marked (series *A* without thread weave, series *B* with double-layer thread weave). In both cases, the polymer filaments were oriented perpendicular to the tensile load axis (i.e. at an angle of 90° to the OX axis). For better contact between the surface of the samples and the grips of the testing equipment, in the first and last layers of the samples of both series, the polymer filaments were also oriented at an angle of 90°.

The method for obtaining the double-layer weave in the designed samples of the *B* series consisted of the alternate laying of polymer filaments in two adjacent layers with the formation of a gap necessary for laying polymer filaments during the reverse movement of the print head (Fig. 1). The dotted lines show the movement of the print head along the corresponding axes of the Cartesian coordinate system. Commands 1.10 and 2.10 are responsible for shifting the print head before repeating path sections 1.1–1.9 and 2.1–2.9.

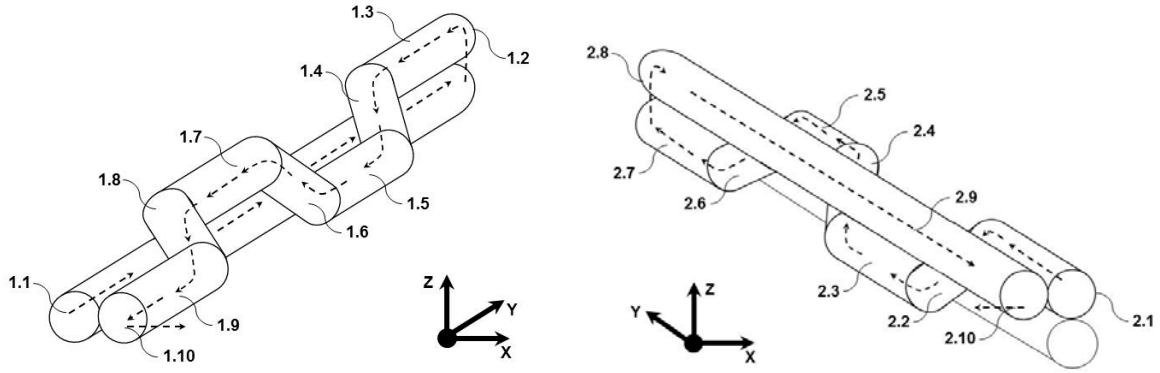

Fig. 1. Method of alternate laying of polymer threads from left to right (a) and right to left (b)

The symbols in the Figure show typical sequential commands in the *G-Code* language, which controlled the movement of the print head along a three-dimensional trajectory. The pseudocode of the algorithm for creating a double-layer weave is shown in Table 1 and contains the specified *G-Code* commands for 3D printing a sample from left to right and right to left. Symbols 1.1–1.10 and 2.1–2.10 in the Table mark the corresponding sections of the trajectory of the print head.

After executing a series of commands 1.1–1.10 in the amount necessary to make a sample from left to right, the print head moved to the height of the second layer. Then the next series of commands 2.1–2.10 was performed to print the sample in the right-to-left direction so that the polymer threads were laid in the resulting gaps. After that, the print head moved to the height of the next layer, and the above process was repeated until the pattern was printed in-depth. The result of the formation of a double-layer weave is shown in Fig. 2.

Table 1. Pseudocode of the 3D printing algorithm for double-layer weave

No.	G-Code commands for 3D printing from left to right	No.	G-Code commands for 3D printing from right to right left
1.1	G1 X0 Y+Y_{11} EE_{11} FF_{11}	2.1	G1 X0 Y+Y_{21} EE_{21} FF_{21}
1.2	G0 Z+ΔZ	2.2	G1 X-X_{22} Y+Y_{22} Z-ΔZ EE_{22} FF_{22}
1.3	G1 X0 Y-Y_{13} EE_{13} FF_{13}	2.3	G1 X0 Y+Y_{23} EE_{23} FF_{23}
1.4	G1 X+X_{14} Y-Y_{14} Z-ΔZ EE_{14} FF_{14}	2.4	G1 X+X_{24} Y+Y_{24} Z+ΔZ EE_{24} FF_{24}
1.5	G1 X0 Y-Y_{15} EE_{15} FF_{15}	2.5	G1 X0 Y+Y_{25} EE_{25} FF_{25}
1.6	G1 X-X_{16} Y-Y_{16} Z+ΔZ EE_{16} FF_{16}	2.6	G1 X-X_{26} Y+X_{26} Z-ΔZ EE_{26} FF_{26}
1.7	G1 X0 Y-Y_{17} EE_{17} FF_{17}	2.7	G1 X0 Y+Y_{27} EE_{27} FF_{27}
1.8	G1 X+X_{18} Y-Y_{18} Z-ΔZ EE_{18} FF_{18}	2.8	G1 Z+ΔZ EE_{28} FF_{28}
1.9	G1 X0 Y-Y_{19} EE_{19} FF_{19}	2.9	G1 X0 Y-Y_{29} EE_{29} FF_{29}
1.10	G1 X+ΔX	2.10	G1 X-ΔX

Fig. 2. Example of the two-layer weave of polymer threads in the right-to-left direction

The main technological parameters of 3D printing of PLA samples are shown in Table 2. The extrusion temperature during printing was chosen close to the melting temperature of PLA plastic. This mode was chosen in order to ensure faster cooling of the material before applying the next layer, as well as to reduce the effect of high melting temperature on the strength properties of the resulting samples.

Table 2. Main technological parameters of FDM 3D printing of PLA plastic samples

No.	Parameter name	Value
1	Print head nozzle diameter	0.4 mm
2	Layer height	0.2 mm
3	Extrusion temperature	185°C
4	Heated platform temperature	60°C
5	Infill	100%
6	Orientation of polymer filaments on the build platform	90° (along OY axis)
7	Orientation of the sample on the platform	0° (along OX axis)

3. Research Methods

In order to confirm the feasibility of 3D printing with alternate laying of a polymer thread in two adjacent layers, the internal structure of the obtained samples was studied. Visual analysis was carried out on Dino-Lite Premier AM7013MZT digital microscope (AnMo Electronics Corporation, Taiwan) with a resolution of 5 MP at 30x magnification.

To assess the effect of the internal structure on the strength of the interlayer bond of the material, the method of static tensile tests was used on Instron 3369 electromechanical tensile testing machine, UK. The essence of the method was to apply a tensile load to the sample until its destruction at a constant temperature and a constant speed of movement of the active grip of the testing equipment equal to 2 mm per minute. Strength tests were carried out at a temperature of 20°C.

The geometrical parameters (width and thickness) of the test samples were measured using an electronic caliper of the ShTsTs-I-125-GOST 166-89 type (ZAO PO Chelyabinsk Instrumental Plant, Russian Federation).

4. Results of the study of strength properties and structure of samples and their discussion

We tested the samples with and without interweaving for tension in the direction across the threads. According to the results of static tests (Table 3), the minimum tensile strength for samples of series *A* turned out to be 32.64 MPa (with an average value of 37.71 MPa).

The digital microscope photograph (Fig. 3) shows that the destruction of the series *A* samples occurred strictly along the line of contact between the melt threads. This type of destruction has already been noted in [13, 23] and is due to the weak bond between the polymer threads.

Table 3. Comparison of static tensile test characteristics for samples with and without weaving

Sample Ref. No.	Sample width b_i, mm	Sample thickness h_i, mm	Maximum load before failure F_{imax}, N	Ultimate tensile strength $\sigma_{bi} = \frac{F_{imax}}{b_i \cdot h_i} 10^{-3}$, MPa	Average tensile strength $\overline{\sigma}_b$, MPa	Standard deviation, S
A1	20.72	2.85	2029.98	34.38	37.71	3.95
A2	20.69	2.85	2336.60	39.63		
A3	20.68	2.87	1937.53	32.64		
A4	20.73	2.86	2464.86	41.57		
A5	20.77	2.89	2422.29	40.35		
B1	20.86	2.85	2465.03	41.46	40.63	0.81
B2	20.79	2.87	2386.50	39.99		
B3	20.90	2.85	2356.21	39.56		
B4	20.89	2.85	2447.88	41.12		
B5	20.89	2.85	2442.62	41.03		

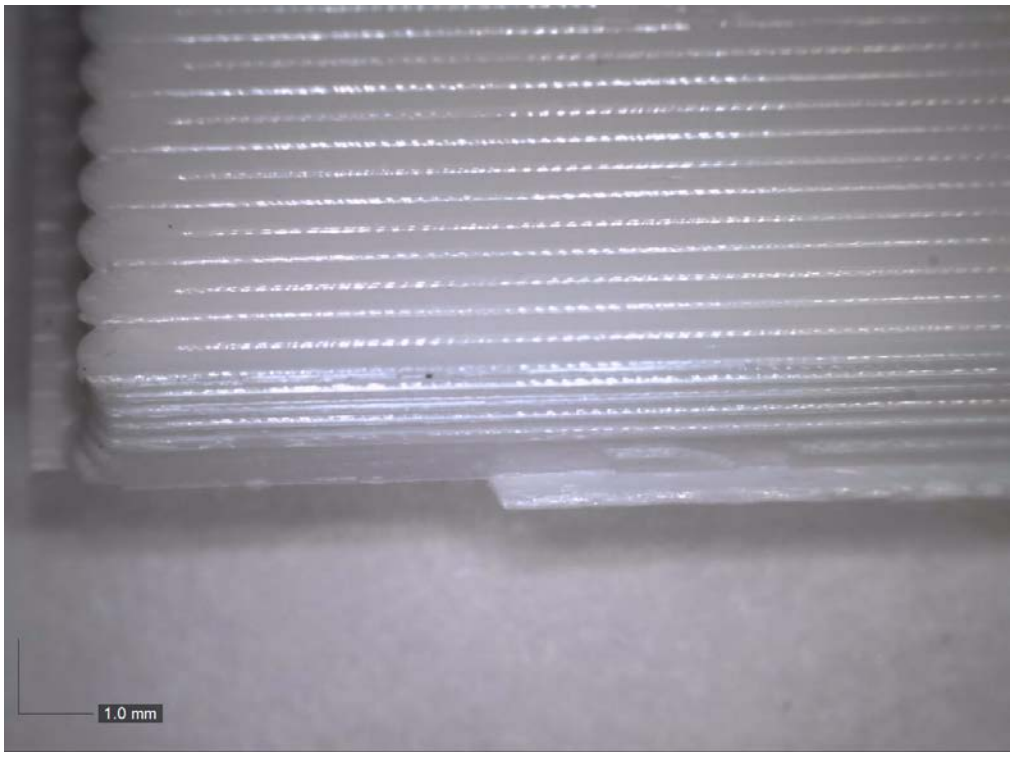

Fig. 3. Fracture surface of A3 sample made of PLA without weave (side view)

The minimum tensile strength for series *B* samples was 39.56 MPa (with an average value of 40.63 MPa). Weave samples have a characteristic transverse fracture pattern (Fig. 4–7).

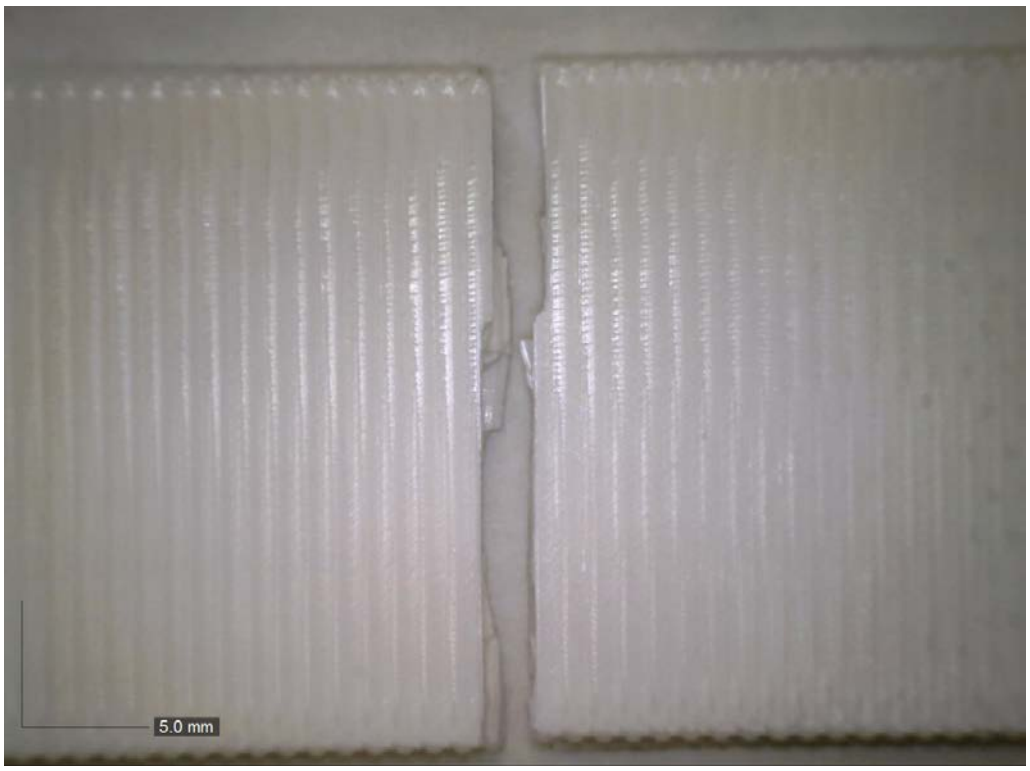

Fig. 4. Fracture surface of B1 sample made of PLA with double-weave (top view)

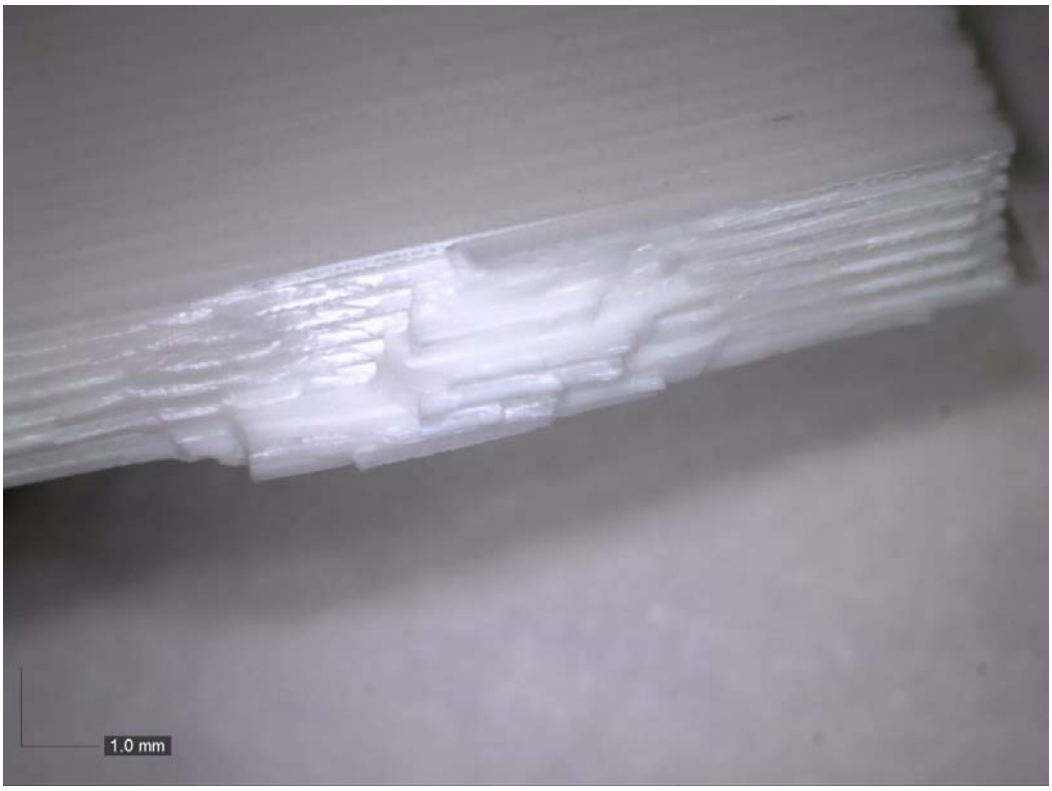

Fig. 5. Fracture surface of B1 sample made of PLA with double-weave (side view)

Fig. 6. Fracture surface of B5 sample made of PLA with double-weave (top view)

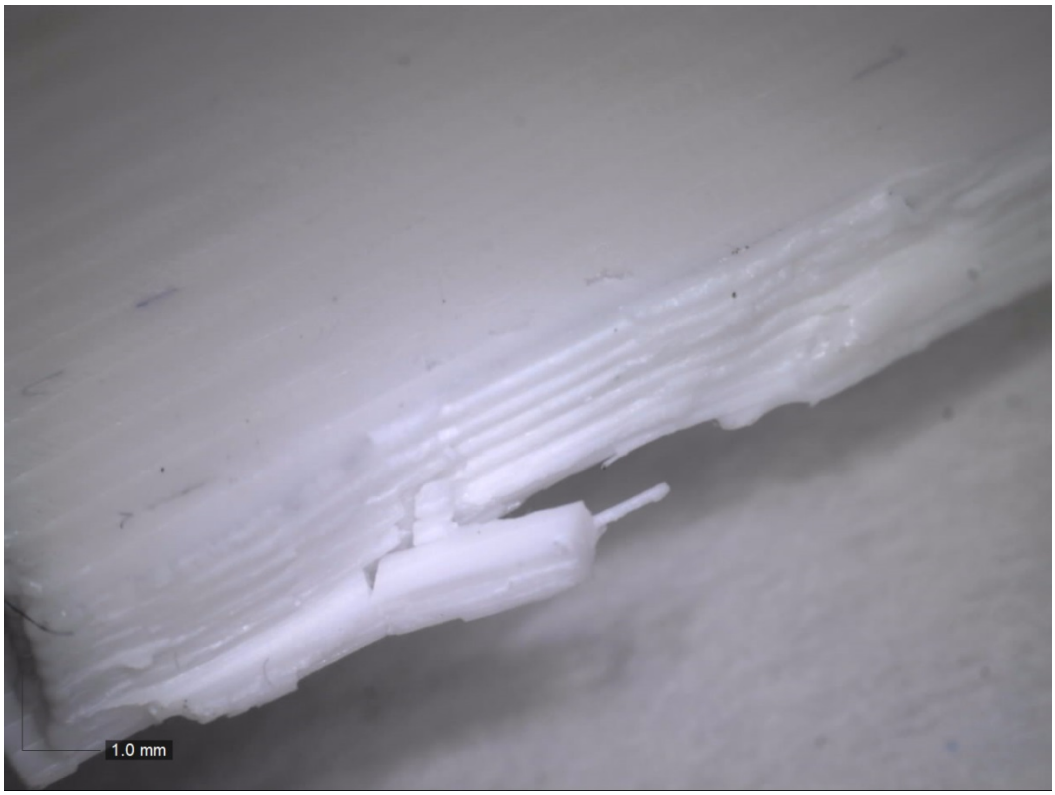

Fig. 7. Fracture surface of B5 sample made of PLA with double-weave (side view)

The results presented above can be supplemented with diagrams of the nominal stress dependence on the strain for samples with and without weaving (Fig. 8). The nominal stress values were calculated as the ratio of the acting load to the cross-sectional area of the samples.

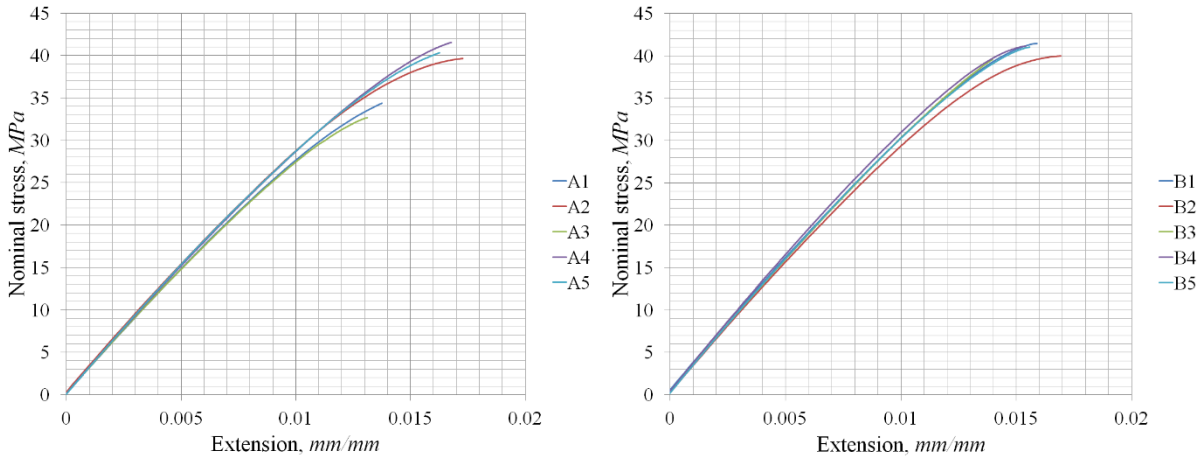

Fig. 8. Diagrams of nominal stress versus strain (extension) for samples with and without weaving

Presented in Table 3 and Fig. 8, the characteristics obtained during static tension of the samples and the typical transverse fracture pattern allow us to draw the following conclusions.

First, the double-layer weave affects the bond strength between the layers of printed PLA samples. Compared to series *A* samples, series *B* samples show an increase in strength from 8% (when comparing average tensile strength values) to 21% (when comparing minimum tensile strength values). The proposed mechanism of influence may be that the double-layer weave prevents a crack from forming along any one line at the polymer

filaments interface. As a result, the direction of propagation of a crack formed in one of the layers of the sample changes when it interacts with the melt threads of the adjacent layer.

Secondly, with a relatively small difference in strength, the value of the standard deviation for samples with the weave turned out to be significantly less than for samples without it. A double-layer weave allows for a smaller variation in tensile strength values relative to the average and, therefore, provides better repeatability and predictability of strength properties.

Thirdly, the double-layer weaving of polymer threads makes it possible to achieve an increase in strength comparable to other methods. A similar result was obtained using the layer height control method. For comparison, when the layer height is halved (from 0.2 to 0.1 mm at a constant nozzle diameter of 0.4 mm), the ultimate strength of the samples increases by 18% [23]. Therefore, the use of double-layer weaves turns out to be the preferred method, as it does not entail an increase in the number of layers and 3D printing time.

Fourthly, the results obtained made it possible to confirm the possibility of 3D printing of samples with a more complex internal structure than in samples with an orientation of 0°, 45°/-45°, 90°, and other directions for laying threads. In a similar way, various variants of multilayer weaves can be implemented.

In addition, we should note an increase in shear resistance of the *B* series samples. When twisted around the longitudinal axis, the two-layered samples of the *A* series broke at angles up to 30°, while the double-layer weave samples could be twisted at an angle exceeding 90°. The degree of influence of the features of the internal structure on the strength properties of FDM products under various types of loading and complexity of weaving is to be determined in subsequent works.

5. Conclusions

The implemented scheme of double-layer weaving of polymer threads influenced the strength of the bond between the layers and the nature of the fracture of the samples obtained by the FDM method.

It is shown that the tensile strength of PLA samples obtained by the FDM method increases from 8% to 21% with a double-layer weave of threads due to strengthening of the bond between the layers of the polymer material. With a relatively small difference in strength values, samples with interweaving have better repeatability of strength properties compared to samples without it. This effect is important in predicting the properties of materials obtained by 3D printing, as well as in designing parts with specified strength properties.

The results obtained indicate that the proposed method, in combination with other methods, can be implemented for polymeric materials and composites based on them and used for local hardening of printed parts, allowing for the requirements of minimum weight, cost, and resistance to environmental factors.

References

[1] Vyavahare S, Teraiya S, Panghal D, Kumar S. Fused deposition modelling: a review. *Rapid Prototyping Journal*. 2020;26(1): 176-201.

[2] Gibson I, Rosen D, Stucker B. *Additive Manufacturing Technologies: Rapid Prototyping to Direct Digital Manufacturing*. NY: Springer; 2015.

[3] Azarov AV, Antonov FK, Golubev MV, Khaziev AR, Ushanov SA. Composite 3D printing for the small size unmanned aerial vehicle structure. *Composites Part B.* 2019;169: 157-163.

[4] Petrova GN, Larionov SA, Platonov MM, Perfilova DN. Thermoplastic materials for new generation for aviation. *Aviation Materials and Technologies*. 2017;S: 420-436.

[5] Lopatin AN, Zverkov ID. Shaping molding tools production for composite parts by means of additive technologies. *Aviation Materials and Technologies*. 2019;2(55): 53-59.
[6] Azarov AV, Latysheva TA, Khaziev AR. Optimal design of advanced 3D printed composite parts of rocket and space structures. *IOP Conference Series: Materials Science and Engineering*. 2020;934: 012062.
[7] Gebisa AW, Lemu HG. Influence of 3D Printing FDM Process Parameters on Tensile Property of ULTEM 9085. *Procedia Manufacturing*. 2019;30: 331-338.
[8] Padovano E, Galfione M, Concialdi P, Lucco G, Badini C. Mechanical and Thermal Behavior of Ultem® 9085 Fabricated by Fused-Deposition Modeling. *Applied Sciences*. 2020;10(9): 3170.
[9] Zanjanijam AR, Major I, Lyons JG, Lafont U, Devine DM. Fused Filament Fabrication of PEEK: A Review of Process-Structure-Property Relationships. *Polymers*. 2020;12(8): 1665.
[10] Cowley A, Perrin J, Meurisse A, Micallef A, Fateri M, Rinaldo L, Bamsey N, Sperl M. Effects of variable gravity conditions on additive manufacture by fused filament fabrication using polylactic acid thermoplastic filament. *Additive Manufacturing*. 2019;28: 814-820.
[11] Prater T, Bean Q, Werkheiser N, Grguel R, Beshears R, Rolin T, Huff T, Ryan R, Ledbetter F, Ordonez E. Analysis of specimens from phase I of the 3D printing in Zero G technology demonstration mission. *Rapid Prototyping Journal*. 2017;23(6): 1212-1225.
[12] Prater T, Werkheiser N, Ledbetter F, Timucin D, Wheeler K, Snyder M. 3D Printing in Zero G Technology Demonstration Mission: complete experimental results and summary of related material modeling efforts. *The International Journal of Advanced Manufacturing Technology*. 2019;101, 391-417.
[13] Ahn SH, Montero M, Odell D, Roundy S, Wright PK. Anisotropic material properties of fused deposition modeling ABS. *Rapid Prototyping Journal*. 2002;8(4): 248-257.
[14] Ziemian C, Sharma M, Ziemian S. Anisotropic Mechanical Properties of ABS Parts Fabricated by Fused Deposition Modelling. In: Gokcek M. (ed.) *Mechanical Engineering*. London: IntechOpen; 2012. p.159-180.
[15] Dey A, Yodo N. A Systematic Survey of FDM Process Parameter Optimization and Their Influence on Part Characteristics. *Journal of Manufacturing and Materials Processing*. 2019;3(3): 64.
[16] Erokhin KS, Gordeev EG, Ananikov VP. Revealing interactions of layered polymeric materials at solid-liquid interface for building solvent compatibility charts for 3D printing applications. *Scientific Reports*. 2019;9: 20177.
[17] Kuznetsov VE, Tavitov AG, Urzhumtsev OD, Mikhalin MV, Solonin AN. Design and Fabrication of Strong Parts from Poly (Lactic Acid) with a Desktop 3D Printer: A Case with Interrupted Shell. *Polymers*. 2019;11(5): 760.
[18] Sun Q, Rizvi GM, Bellehumeur CT, Gu P. Effect of processing conditions on the bonding quality of FDM polymer filaments. *Rapid Prototyping Journal*. 2008;14(2): 72-80.
[19] Bellehumeur C, Li L, Sun Q, Gu P. Modeling of Bond Formation Between Polymer Filaments in the Fused Deposition Modeling Process. *Journal of Manufacturing Processes*. 2004;6(2): 170-178.
[20] Onwubolu GC, Rayegani F. Characterization and Optimization of Mechanical Properties of ABS Parts Manufactured by the Fused Deposition Modelling Process. *International Journal of Manufacturing Engineering*. 2014;2014: 598531.
[21] Spoerk M, Arbeiter F, Cajner H, Sapkota J, Holzer C. Parametric optimization of intra- and inter-layer strengths in parts produced by extrusion-based additive manufacturing of poly(lactic acid). *Journal of Applied Polymer Science*. 2017;134(41): 45401.
[22] Slonov AL, Khashirov AA, Zhansitov AA, Rzhevskaya EV, Khashirova SY. The influence of the 3D-printing technology on the physical and mechanical properties of polyphenylene sulfone. *Rapid Prototyping Journal*. 2018;24(7): 1124-1130.

[23] Kuznetsov VE, Solonin AN, Urzhumtsev OD, Schilling R, Tavitov AG. Strength of PLA Components Fabricated with Fused Deposition Technology Using a Desktop 3D Printer as a Function of Geometrical Parameters of the Process. *Polymers*. 2018;10(3): 313.
[24] Aliheidari N, Christ J, Tripuraneni R, Nadimpalli S, Ameli A. Interlayer adhesion and fracture resistance of polymers printed through melt extrusion additive manufacturing process. *Materials & Design*. 2018;156: 351-361.
[25] Liu Z, Wang Y, Wu B, Cui C, Guo Y, Yan C. A critical review of fused deposition modeling 3D printing technology in manufacturing polylactic acid parts. *The International Journal of Advanced Manufacturing Technology*. 2019;102: 2877-2889.
[26] Polyakov IV, Vaganov GV, Yudin VE, Smirnova NV, Ivan'kova EM, Popova EN. Study of Polyetherimide and Its Nanocomposite 3D Printed Samples for Biomedical Application. *Polymer Science, Ser. A*. 2020;62: 337-342.

THE AUTHOR

Pogrebnoi A.V.
e-mail: a.v.pogrebnoy@yandex.ru
ORCID: 0000-0001-7296-5387